

Quasi-Geostrophic Waves in a Stratified Ocean with Bottom Topography

NOBUO SUGINOHARA¹

Department of Oceanography, Florida State University, Tallahassee, FL 32306

(Manuscript received 23 July 1979, in final form 8 October 1980)

ABSTRACT

Quasi-geostrophic waves in a two-layer ocean with bottom topography on a β -plane are examined in detail. The bottom slopes in an arbitrary direction but gently and uniformly. A clear understanding of vertical normal modes is obtained from the use of the "upper layer component" and the "lower layer component" as a basic concept, where the upper layer component (ULC) and the lower layer component (LLC) are motions confined to the upper and the lower layers, respectively, and are independent of each other. Modification of the normal modes from ULC and LLC is measured by the effect of divergence which couples upper and lower layer motions. The effect of bottom topography tends to suppress the coupling. The extent to which the effect of topography suppresses the coupling depends on the thickness ratio and relative effects of the planetary and topographic β as well as the horizontal scale of waves relative to the internal radius of deformation. In some realistic circumstances, the upper layer mode is isolated completely from the bottom and the lower layer mode is trapped completely by the bottom even for waves whose wavelength is much longer than the internal deformation radius. When the phase speeds of the ULC and LLC are identical, resonance takes place and induces an interchange of their properties. Occurrence of resonance is typical for a general orientation of bottom topography.

1. Introduction

In a stratified, flat-bottom ocean on a β -plane, the barotropic and baroclinic modes are the natural vertical normal modes. The vertical structure of horizontal velocities associated with waves of those modes is determined independently of wavenumber and frequency. This leads to a clear understanding of the properties of the barotropic and baroclinic Rossby (planetary) waves. However, when the bottom slopes, the direct use of the barotropic and baroclinic modes is no longer possible. Inapplicability of this well-known idea makes any problem difficult to interpret.

For topography with gentle slope oriented east-west, Rhines (1970) obtained normal modes and pointed out the existence of bottom and surface modes. The essential properties of the two modes may be roughly described as follows. In a two-layer system, the bottom mode is characterized by the dominance of lower layer motion, and propagation is controlled by both the topographic and planetary β . For the surface mode, the motion is isolated away from the bottom and propagation is controlled mainly by the planetary β . The vertical structure and propagation of the normal modes depend strongly on the horizontal scale of the waves. As the scale becomes small compared with the deformation radius, the

characteristics (trapping and isolation) become more typical. In a continuously stratified system (essentially for the case in which isopycnals meet the sloped bottom), buoyancy plays an important role for waves shorter than the internal deformation radius, and buoyancy cutoff takes place.

The nature of the vortex may manifest the vertical structure of the normal modes. The fact that the trapping and isolation depend on the horizontal scale of the vortex relative to the internal deformation radius is natural, as was noted by Prandtl (1952). However, dependence of the characteristics on other parameters such as the orientation of bottom topography is not obvious.

In the present paper, quasi-geostrophic waves in a stratified ocean with bottom topography on a β -plane are examined in detail. The bottom slopes in an arbitrary direction, but gently and uniformly. A density stratification is assumed to be represented by two homogeneous layers. A two-layer model retains the essential dynamics of a stratified ocean unless the thermocline intersects the sloped bottom (the buoyancy oscillation is not considered in a two-layer model). Vorticity equations for the upper and lower layers are suitable for describing large-scale and low-frequency waves such as the planetary and topographic (Rossby) waves. Motions of the two layers are coupled by the effect of divergence. Rhines' results suggest that the normal modes retain the characteristics of the decoupled case, i.e., they

¹ Permanent affiliation: Geophysical Institute, University of Tokyo, Bunkyo-ku, Tokyo 113, Japan.

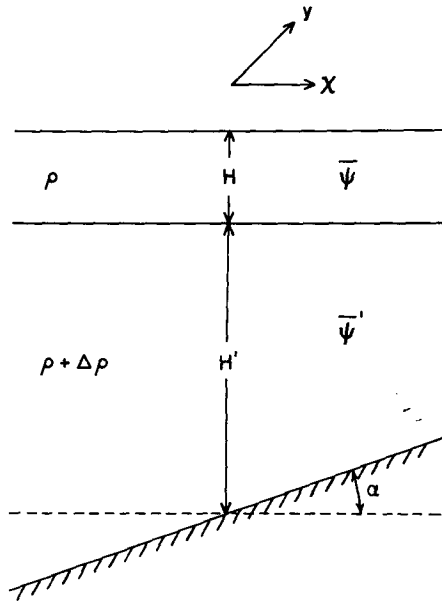


FIG. 1. The model geometry.

are the upper layer and lower layer modes. The coupling between the upper and lower layers (effect of divergence) tends to be suppressed by the effect of bottom topography. Therefore, the normal modes in a two-layer ocean with bottom topography will be considered in terms of motion confined to the upper layer and motion confined to the lower layer.

2. Formulation and mechanical analog

We consider quasi-geostrophic waves in a two-layer ocean with a rigid top and a uniformly sloped bottom on a β -plane (Fig. 1). We take the right-handed coordinate system fixed in the topography with y parallel to isobaths and x normal to isobaths (positive for upslope). Thus, the depth is taken to vary only with x ; the expression for the thickness of the lower layer is $H' - \alpha x$. The Coriolis parameter is then given by

$$f = f_0 + \beta^a y + \beta^c x,$$

where $\beta^a = \beta \cos \theta$ and $\beta^c = \beta \sin \theta$, where $\theta (< 2\pi)$ is the angle measured counterclockwise from the east to the x axis.

The quasi-geostrophic motions are only slightly divergent and allow the use of a streamfunction for the upper and lower layers, i.e.,

$$\begin{pmatrix} \bar{\psi}_x = v, \\ \bar{\psi}_y = -u, \end{pmatrix} \quad \begin{pmatrix} \bar{\psi}'_x = v', \\ \bar{\psi}'_y = -u', \end{pmatrix}$$

where the subscript $x(y)$ denotes the derivative with respect to $x(y)$ and the variables without (with) primes denote those for the upper (lower) layer. Now we

assume that the slope is gentle, $\alpha x/H' (= \delta) \ll 1$ as well as $\beta^c x/f_0 \ll 1$ and $\beta^a y/f_0 \ll 1$, where αx is the fractional change in the lower layer thickness. Then the effect of bottom topography is retained only in the vortex stretching terms, and the linearized vorticity equations for the upper and lower layers may be written

$$\{\nabla^2 \bar{\psi} + F(\bar{\psi}' - \bar{\psi})\}_t + \beta^a \bar{\psi}_x - \beta^c \bar{\psi}_y = 0, \quad (2.1a)$$

$$\{\nabla^2 \bar{\psi}' + F'(\bar{\psi} - \bar{\psi}')\}_t + \beta^a \bar{\psi}'_x - \beta^c \bar{\psi}'_y - \beta^T \bar{\psi}'_y = 0, \quad (2.1b)$$

where

$$F = \frac{f_0^2}{\Delta \rho g H}, \quad F' = \frac{f_0^2}{\Delta \rho g H'},$$

t is time and $\beta^T = f_0 \omega/H'$. A formal derivation of the vorticity equations from the momentum and continuity equations is given by Rhines (1977). Motions of the upper and lower layers are coupled by the effect of divergence. It should be noted that for motions for which the horizontal scale is much smaller than the internal deformation radius ($F^{-1/2}$ and $F'^{-1/2}$), the divergence terms can be ignored, and motions of the two layers become independent of each other.

We now consider plane-wave solutions in Eqs. (2.1). Putting

$$\begin{pmatrix} \bar{\psi} \\ \bar{\psi}' \end{pmatrix} = \begin{pmatrix} \psi(x) \\ \psi'(x) \end{pmatrix} \exp[i(l y - \omega t)] \exp[-i(\beta^a/2\omega)x]$$

into Eqs. (2.1a, b), where $\omega (\ll f_0 \delta)$ is angular frequency and l wavenumber in the y direction, we obtain equations in terms of $\psi(x)$ and $\psi'(x)$:

$$\psi_{xx} + A\psi + F(\psi' - \psi) = 0, \quad (2.2a)$$

$$\psi'_{xx} + (A + B)\psi' + F'(\psi - \psi') = 0, \quad (2.2b)$$

where

$$A = -l^2 + \frac{\beta^c}{\omega} l + \left(\frac{\beta^a}{2\omega}\right)^2,$$

$$B = \frac{\beta^T}{\omega} l.$$

The above equations yield an analogous form for a coupled harmonic oscillator problem. An intuitive understanding may be obtained from this mechanical analog. The natural wavenumbers k in the cross-isobath direction, for the case where the upper and lower layers are decoupled, may be given as follows:

$$\begin{aligned} \left(k_u + \frac{\beta^a}{2\omega}\right)^2 &= A - F \\ &= -\left(l - \frac{\beta^c}{2\omega}\right)^2 + \left(\frac{\beta^a}{2\omega}\right)^2 + \left(\frac{\beta^c}{2\omega}\right)^2 - F \end{aligned}$$

or

$$\omega = \frac{-\beta^a k_u + \beta^c l}{k_u^2 + l^2 + F} \quad \text{for the upper layer,} \quad (2.3a)$$

$$\begin{aligned} \left(k_l + \frac{\beta^a}{2\omega}\right)^2 &= A + B - F' \\ &= -\left(l - \frac{\beta^c}{2\omega} - \frac{\beta^T}{2\omega}\right)^2 + \left(\frac{\beta^a}{2\omega}\right)^2 \\ &\quad + \left(\frac{\beta^c}{2\omega}\right)^2 + \left(\frac{\beta^T}{2\omega}\right)^2 + \frac{2\beta^c\beta^T}{(2\omega)^2} - F' \end{aligned}$$

or

$$\omega = \frac{-\beta^a k_l + \beta^c l + \beta^T l}{k_l^2 + l^2 + F'} \quad \text{for the lower layer.} \quad (2.3b)$$

These provide dispersion relations for waves whose motion is confined completely to the upper layer or to the lower layer. We name these independent motions of the upper and lower layers the ‘‘upper layer component’’ (ULC) and the ‘‘lower layer component’’ (LLC). Propagation of the ULC and LLC is obvious from their vertical structures: planetary (Rossby) waves for ULC and combined planetary and topographic waves for LLC. It is noted that the dispersion curves for ULC and LLC are portrayed by circles in the wavenumber plane with fixed frequency. According to Eqs. (2.2a,b), the strength of coupling between the upper and lower layers may be represented by

$$C = \frac{4FF'}{(F - F' + B)^2}. \quad (2.4)$$

$C \ll 1$ yields a very weak coupling and is realized when $F'/F \approx 1$ (or $H/H' \approx 1$). The effect of bottom topography (the term B) tends to suppress the coupling. When the denominator is zero, i.e., $F - F' + B = 0$, resonance takes place. Occurrence of resonance is visualized in the wavenumber plane and the dispersion diagram as intersections of the dispersion curves for ULC and LLC, which indicate that the phase speeds of ULC and LLC are identical.

3. Normal modes for some typical bottom topography orientations

In this section, normal modes are obtained numerically. Seeking combination, $\Phi_m = \psi + S_m\psi'$, $m = 1, 2$, in Eqs. (2.2), we may obtain two equations in terms of Φ_m and S_m :

$$F'S_m^2 + (F' - F - B)S_m - F = 0, \quad (3.1a)$$

$$\Phi_{m,xx} + (A + F'S_m - F)\Phi_m = 0, \quad m = 1, 2. \quad (3.1b)$$

Looking for periodic solutions in the cross-isobath direction, $\Phi_m \sim e^{i\mu x}$ yields

$$\mu^2 = A + F'S_m - F.$$

The wavenumber in the cross-isobath direction is given by

$$k = -\frac{\beta^a}{2\omega} \pm \mu.$$

Then, a dispersion relation for mode m may become

$$k^2 + \frac{\beta^a}{\omega}k + l^2 - \frac{\beta^c}{\omega}l - F'S_m + F = 0. \quad (3.1c)$$

The S_m describes the vertical structure

$$S_m = \left(\frac{\psi_0'}{\psi_0}\right)_m \frac{F}{F'} = \left(\frac{\psi_0'}{\psi_0}\right)_m \frac{H'}{H}, \quad m = 1, 2. \quad (3.2)$$

For numerical demonstration, we consider three cases of bottom topography orientation: $\theta = 90^\circ$ (upslope to the north), $\theta = 270^\circ$ (upslope to the south) and $\theta = 0^\circ$ (upslope to the east). These cases will yield typical examples for coexistence of the planetary and topographic β . For each of the three cases, we compare the strength of coupling by taking $H/H' = 1/14$ and $2/3$ with fixed total depth $H + H' = 3000$ m.

In the following figures, wavenumbers and frequency are scaled by

$$\left(\frac{\hat{k}}{\hat{l}}\right) = \left(\frac{k}{l}\right) \frac{(\Delta\rho g H)^{1/2}}{f_0} \quad \text{and} \quad \hat{\omega} = \frac{\omega}{f_0}.$$

The deformation radius for the upper layer is used as the length scale. With $H + H' = 3000$ m and $\Delta\rho = 2 \times 10^{-3}$ g cm⁻³, the deformation radius at 30° latitude is 27.5 km for $H/H' = 1/14$ ($H = 200$ m) and 67.4 km for $H/H' = 2/3$ ($H = 1200$ m). $\hat{k} = \hat{l} = 1$, which refers to the deformation radius, yields a different real distance for each of the two cases. This scaling may be optimum for describing phenomena controlled by the scale relative to each of the deformation radii.

a. Upslope to the north ($\theta = 90^\circ$)

The planetary and topographic β are in the same direction: $\beta^c = \beta$, $\beta^a = 0$ and $\beta^T = \beta^c = \beta$. For this orientation of bottom topography, no resonance takes place unless $F < F'(H > H')$ as observed in the dispersion curves for ULC and LLC [Eqs. (2.3a,b)] in the wavenumber plane. The dispersion curves of the normal modes as well as of ULC and LLC in the (\hat{k}, \hat{l}) plane with $\hat{\omega} = 0.002$ (1-year period) are plotted in Fig. 2a for $H/H' = 1/14$ and in Fig. 2b for $H/H' = 2/3$. The vertical structure which is a function of \hat{l} is sketched on each of the curves. In Fig. 2a ($H/H' = 1/14$), no difference in the dispersion curves between the normal modes and ULC and LLC is found in the whole domain. However, a close examination shows that a slight modification

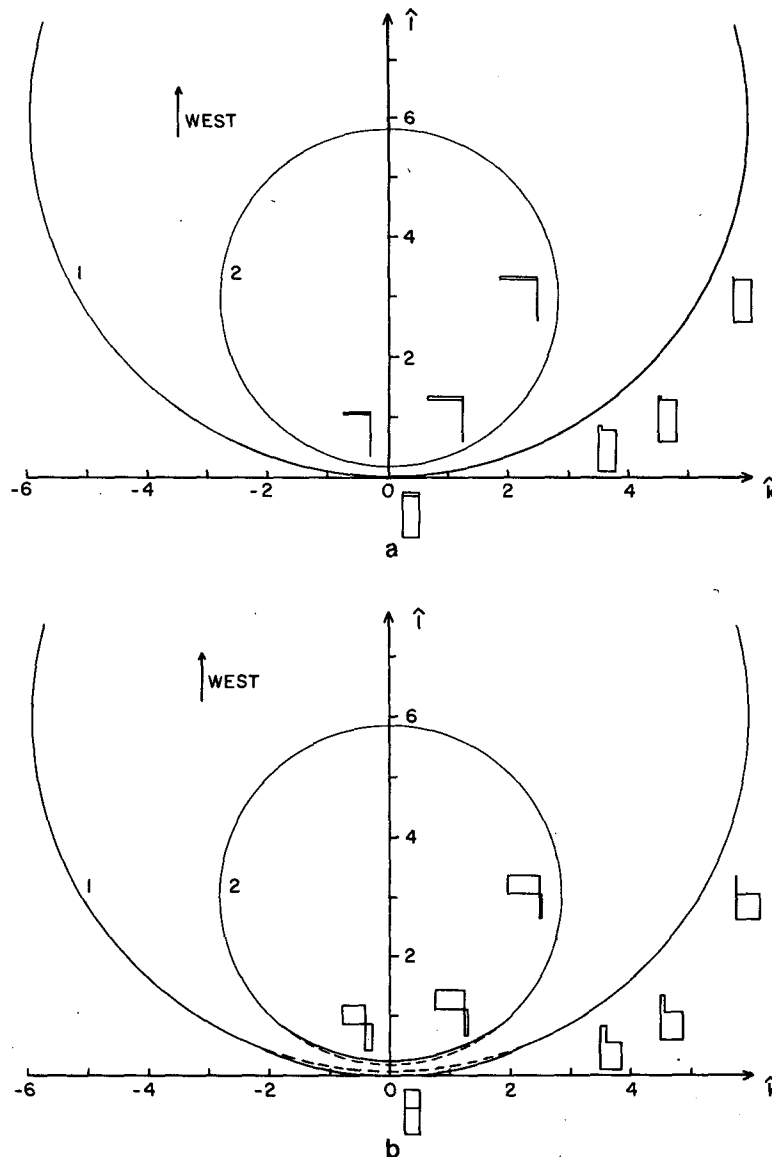


FIG. 2. Dispersion curves of the normal modes and ULC and LLC in the (\hat{k}, \hat{l}) plane with $\hat{\omega} = 0.002$ for $\theta = 90^\circ$: (a) $H/H' = 1/14$, (b) $H/H' = 2/3$. The dashed lines are for ULC and LLC. The sketches show vertical structure. $\beta^T = \beta = 2 \times 10^{-13} \text{ cm}^{-1} \text{ s}^{-1}$.

of mode 1 (the lower layer mode) from LLC occurs in the range very close to wavenumber $(\hat{k}^2 + \hat{l}^2)^{1/2} = 0$ as the vertical structure suggests (no effect of bottom topography at $\hat{l} = 0$). For $H/H' = 2/3$ (Fig. 2b), modification of the normal modes is found in the range of small wavenumbers but not to such a conspicuous extent, and decreases rapidly as wavenumber increases. For large wavenumbers no difference in the dispersion curves is found, and the vertical structure shows the properties of ULC and LLC. The ratio H/H' accounts for the modification. As H/H' approaches unity, the modification devel-

ops. But the range where the normal modes are modified by the coupling is limited to relatively small values of wavenumber, i.e., $(\hat{k}^2 + \hat{l}^2)^{1/2} < 1$.

To demonstrate dependence of the modification on $\hat{\omega}$ and \hat{l} , the dispersion diagrams of the normal modes and ULC and LLC in the $(\hat{\omega}, \hat{l})$ plane with $\hat{k} = 0.5$ are plotted in Fig. 3 for $H/H' = 2/3$. The vertical structure which is a function of $\hat{\omega}$ and \hat{l} is sketched on each of the curves. It is clearly seen that the effect of decreasing $\hat{\omega}$ and increasing \hat{l} are to weaken the coupling as understood from (2.4). For the lower mode (mode 1), considerable modification

is observed for high frequency and small wave-number.

For the upper layer mode (mode 2), modification is not as conspicuous as that for the lower layer mode. The vertical structure indicates that the upper layer mode possesses the property of ULC in the whole range of \hat{l} .

For $H/H' = 1/14$ for waves of higher frequency, only a slight modification is observed.

b. Upslope to the south ($\theta = 270^\circ$)

The planetary and topographic β are in the opposite direction: $\beta^c = -\beta$, $\beta^a = 0$ and $\beta^T = -2\beta^c = 2\beta$. In this orientation of bottom topography, no resonance takes place for $\beta^T > \beta$. The dispersion curves in the (\hat{k}, \hat{l}) plane with $\hat{\omega} = 0.002$ are plotted in Fig. 4a for $H/H' = 1/14$ and in Fig. 4b for $H/H' = 2/3$. There exists only one normal mode (mode 1): the mode in which the two layers oscillate in phase as seen in the vertical structure. Absence of the other mode (mode 2) may be understood from the mechanical analog. The ratio H/H' accounts for modification. No difference between the normal modes and ULC and LLC is found in Fig. 4a (ULC and the upper layer mode in $\hat{l} < 0$, and LLC and the lower layer mode in $\hat{l} > 0$).

In Fig. 5, the dispersion diagram with $\hat{k} = 0.5$ is plotted for $H/H' = 2/3$. For waves of higher frequency, modification is observed but not to such a remarkable extent as that in Fig. 3. Even for $|\hat{l}| < 1$, the normal modes show the properties of ULC and LLC as seen in the vertical structure.

c. Upslope to the east ($\theta = 0^\circ$)

The planetary and topographic β are at the right angles: $\beta^c = 0$, $\beta^a = \beta$ and $\beta^T = \beta$. This case yields a typical example for occurrence of resonance. The dispersion curves in the (\hat{k}, \hat{l}) plane with $\hat{\omega} = 0.002$ are plotted in Fig. 6a for $H/H' = 1/14$ and in Fig. 6b for $H/H' = 2/3$. Resonance takes place in both cases as found in intersections of the curves for ULC and LLC. Interchange of their properties (ULC and LLC) between the normal modes is clearly observed. Even for the case with resonance, the ratio H/H' also accounts for modification. As H/H' approaches unity, modification by resonance becomes larger. Modification caused by the resonance in Figs. 6a and 6b is larger than that for the cases without resonance (cf. Fig. 6a with Fig. 2a and Fig. 4a, and Fig. 6b with Fig. 2b and Fig. 4b). It should be remarked that even for $H/H' = 2/3$, modification is confined to the range near resonance, and the normal modes retain the properties of ULC and LLC.

For higher frequency waves, modification by resonance is larger. In the numerical demonstration, special attention is not paid to dependence of the

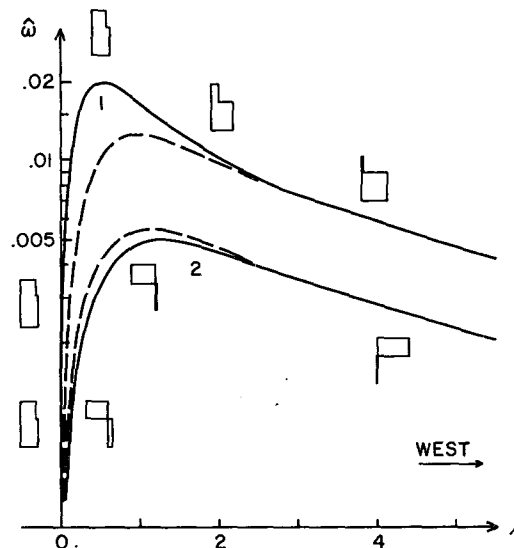


FIG. 3. Dispersion diagram with $\hat{k} = 0.5$ for $H/H' = 2/3$ and $\theta = 90^\circ$. The dashed lines are for ULC and LLC.

coupling on the value of β^T . A role of β^T will be discussed in terms of relative effects of β^T and β in Section 4.

In conclusion, the normal modes retain the properties of ULC and LLC no matter how strong the coupling is and even for the case with resonance. The introduction of ULC and LLC may be suitable for describing the properties of the normal modes.

4. Relative effects of the planetary and topographic β

In this section, special attention is paid to the relative effects of the planetary and topographic β on the coupling between the two layers (trapping and isolation).

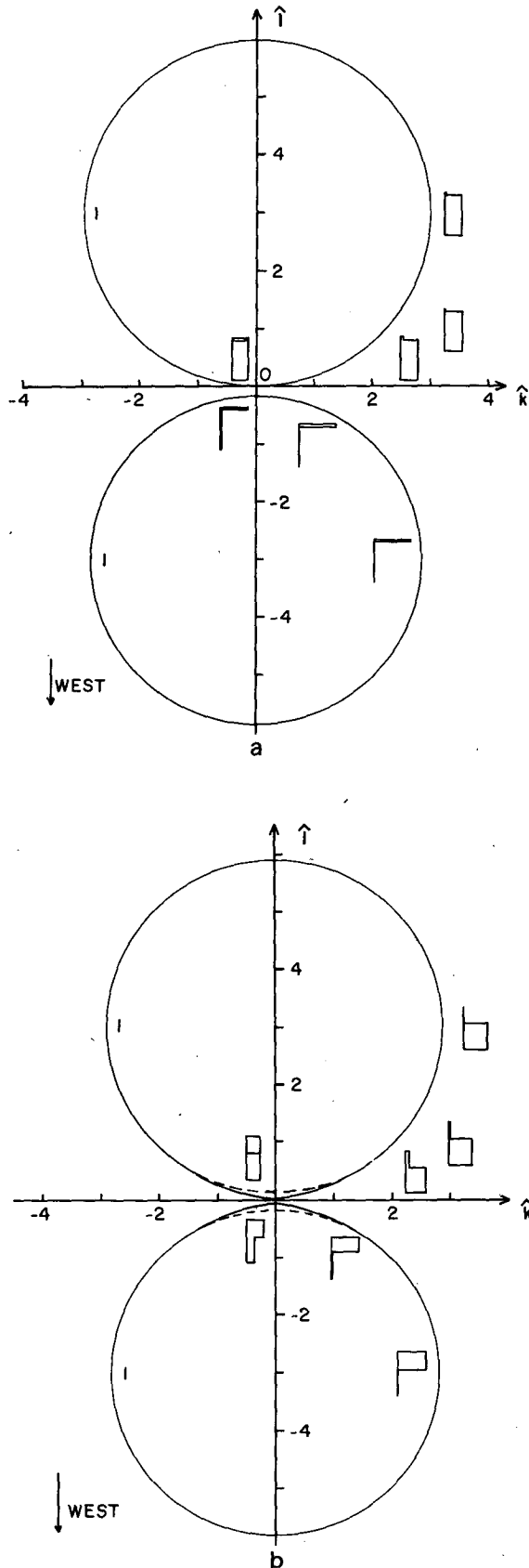
First, to clarify these effects we will obtain analytical expressions for normal modes in the two extreme cases, $\beta = 0$ and $\beta^T \gg \beta$. Let us consider a case where bottom topography is oriented east-west ($\theta = 90^\circ$ or 270°) and $H < H'$, which avoids occurrence of resonance. We look for plane-wave solutions,

$$\begin{pmatrix} \bar{\psi} \\ \psi' \end{pmatrix} = \begin{pmatrix} \psi_0 \\ \psi_0' \end{pmatrix} e^{i(kx + ly - \omega t)}$$

in Eqs. (2.1). Then Eqs. (2.1a,b) become

$$-(k^2 + l^2)\psi_0 + \frac{\beta^c}{\omega} l\psi_0 + F(\psi_0' - \psi_0) = 0, \quad (4.1a)$$

$$\begin{aligned} & -(k^2 + l^2)\psi_0' + \frac{\beta^c}{\omega} l\psi_0' \\ & + \frac{\beta^T}{\omega} l\psi_0' + F(\psi_0 - \psi_0') = 0. \quad (4.1b) \end{aligned}$$



The above equations yield a quadratic in terms of ω , i.e.,

$$K^2(K^2 + F + F')\omega^2 - l[\beta^c(2K^2 + F + F') + \beta^T(K^2 + F)]\omega + \beta^c l^2(\beta^c + \beta^T) = 0, \quad (4.2)$$

where $K^2 = k^2 + l^2$.

(i) $\beta = 0 (\beta^T \neq 0).$

$$\omega = \frac{\beta^T l}{K^2 + F' \left(1 - \frac{F}{K^2 + F}\right)},$$

$$\frac{\psi_0'}{\psi_0} = \frac{K^2 + F}{F}, \quad (4.3a)$$

$$\omega = 0. \quad (4.3b)$$

One of the normal modes shows a steady solution. The other mode is a topographic wave affected by stratification. The characteristic of this wave depends on the scale relative to the deformation radius $F^{-1/2}$. For small wavenumber, $K^2 \ll F$, this wave becomes a barotropic topographic wave. The coupling (the vertical structure represents its strength) does not depend on the value of β^T as seen in (4.3a) and (2.4).

(ii) $\beta^T \gg \beta.$

$$\omega = \frac{\beta^T l + \beta^c \left\{1 + \frac{FF'}{(K^2 + F)^2}\right\} l}{K^2 + F' \left(1 - \frac{F}{K^2 + F}\right)},$$

$$\frac{\psi_0'}{\psi_0} = \frac{(K^2 + F)^2}{F \left(K^2 + F + \frac{\beta^c}{\omega} l\right)}, \quad (4.4a)$$

$$\omega = \frac{\beta^c l}{K^2 + F},$$

$$\frac{\psi_0'}{\psi_0} = \frac{F' \left(K^2 + F + \frac{\beta^c}{\omega} l\right)}{(K^2 + F)^2} \sim 0, \quad (4.4b)$$

where

$$\beta^c = \begin{cases} \beta & \text{for } \theta = 90^\circ \\ -\beta & \text{for } \theta = 270^\circ. \end{cases}$$

Inclusion of the planetary β creates a wave mode which is isolated from the bottom as seen in (4.4b). This case represents the typical relative effects of the planetary and topographic β on the upper layer mode.

FIG. 4. Dispersion curves of the normal modes and ULC and LLC in the (k, l) plane with $\hat{\omega} = 0.002$ for $\theta = 270^\circ$: (a) $H/H' = 1/14$, (b) $H/H' = 2/3$. $\beta^T = 2\beta$.

For the lower layer mode [Eq. (4.4a)] the vertical structure indicates that the extent to which motion is confined to the lower layer depends on the planetary β as well as the scale relative to the deformation radius [compare with (4.3a)]. The dispersion relation (4.4a) indicates that frequency shift from that of a topographic wave (for $\beta = 0$) is caused by a planetary wave. The sign depends on the orientation of bottom topography. For waves propagating eastward (westward), frequency is decreased (increased) by the effect of β for given k and l . The decrease (increase) in frequency leads to stronger (weaker) trapping of the lower layer mode by the bottom compared with that on an f plane for given k and l with fixed β^T as seen in (2.4). This suggests that the orientation of bottom topography plays an important role on the coupling.

Now we discuss the relative effects of the planetary and topographic β on the coupling for a general case.

To understand the lower layer mode, we plot the dispersion diagrams in the $(\hat{\omega}, \hat{k})$ plane with $l = 0.5$ for $\beta = 0$, $\beta/\beta^T = 1/5$ and 1 with fixed β^T in Fig. 7 for $\theta = 0^\circ$ (upslope to the east) and $H = 500$ m, $H' = 2500$ m

$$\begin{pmatrix} \hat{k} \\ l \end{pmatrix} = \begin{pmatrix} k \\ l \end{pmatrix} \frac{(\Delta\rho g H)^{1/2}}{f_0} \quad \text{and} \quad \hat{\omega} = \frac{\omega}{f_0} .$$

The vertical structure sketched is a function of $\hat{\omega}$ when β^T is fixed ($\beta^T = 2 \times 10^{-13} \text{ cm}^{-1} \text{ s}^{-1} = \beta$). It is clearly observed that $\hat{\omega}$ is decreased for $\hat{k} > 0$ (waves propagating eastward) and increased for $\hat{k} < 0$ (propagating westward) by the effect of β . As β/β^T increases, the above characteristic becomes typical. This may account for weakening or strengthening of the coupling compared with that on an f plane for given k and l with fixed β^T as seen in (2.4). It should be noted that the ratio β/β^T plays the same role as that discussed above, when β^T , instead of β , is changed as it is in real oceans. Frequency is not simply proportional to β^T on a β plane as it is on an f plane [see (4.3a)] for given k and l , because a simple expression for a dispersion relation like (4.4a) is not obtained in general cases.

For $\theta = 180^\circ$ (downslope to the east), a decrease in frequency compared with that on an f plane is also observed for waves propagating eastward. Therefore, for waves propagating eastward, the combined effect of β and β^T gives rise to a strong trapping of the lower layer mode by the bottom, even for waves longer than the deformation radius.

To understand the relative effects of β and β^T on the upper layer mode, the dispersion diagrams in the $(\hat{\omega}, \hat{k})$ plane with $l = 0.5$ for $\beta/\beta^T = 1/5$ and 1 with fixed β^T are plotted in Fig. 8 (parameters are the same as in Fig. 7). The vertical structure sketched is a function of $\hat{\omega}$. It is clearly demonstrated that $\hat{\omega}$ decreases as β becomes smaller than β^T . This ac-

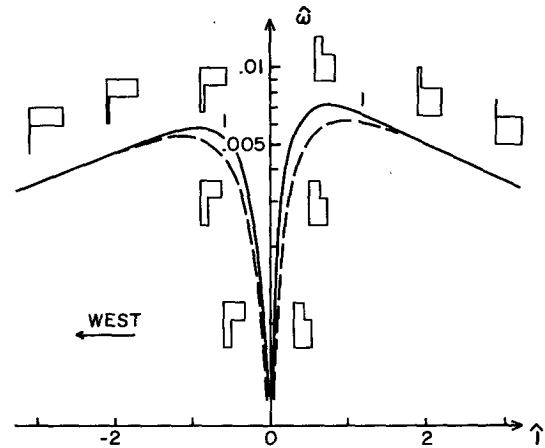


FIG. 5. Dispersion diagram with $\hat{k} = 0.5$ for $H/H' = 2/3$ and $\theta = 270^\circ$.

counts for the weakening of the coupling for the upper layer mode for given \hat{k} and l as seen in (2.4). Therefore, as β/β^T decreases, isolation from the bottom becomes more typical. For $\beta/\beta^T \ll 1$, complete isolation of the upper layer mode from the bottom takes place even for waves much longer than the deformation radius [also see (4.4b)]. Unless $\beta^T \ll \beta$ and $|\beta^T l/\omega| \ll |F - F'|$, the coupling does not depend on the orientation of bottom topography as understood from the equation for the upper layer (no direct effect of bottom topography on the upper layer).

5. Discussion and conclusion

The properties of waves in a two-layer ocean with bottom topography on a β -plane have been presented in detail. To represent independent motions of the upper and lower layers, the upper and lower layer components are introduced. Upper and lower layer motions are coupled by the effect of divergence. The strength of coupling is measured by the relative effects of bottom topography and divergence, (2.4). The effect of bottom topography tends to suppress the coupling. The extent to which the effect of topography suppresses the coupling depends on the thickness ratio and the relative effects of the planetary and topographic β as well as the scale of waves relative to the deformation radius. For $H/H' \ll 1$, the normal modes are quite similar to ULC and LLC even for waves much longer than the deformation radius. The effects of the planetary and topographic β play different roles on the upper and lower layer modes. For the upper layer modes, a decrease in the ratio β/β^T accounts for the weakening of the effect of coupling. When $\beta/\beta^T \ll 1$, complete isolation from the bottom takes place even for waves much longer than the deformation radius. For the lower layer mode, the decrease in β/β^T does not

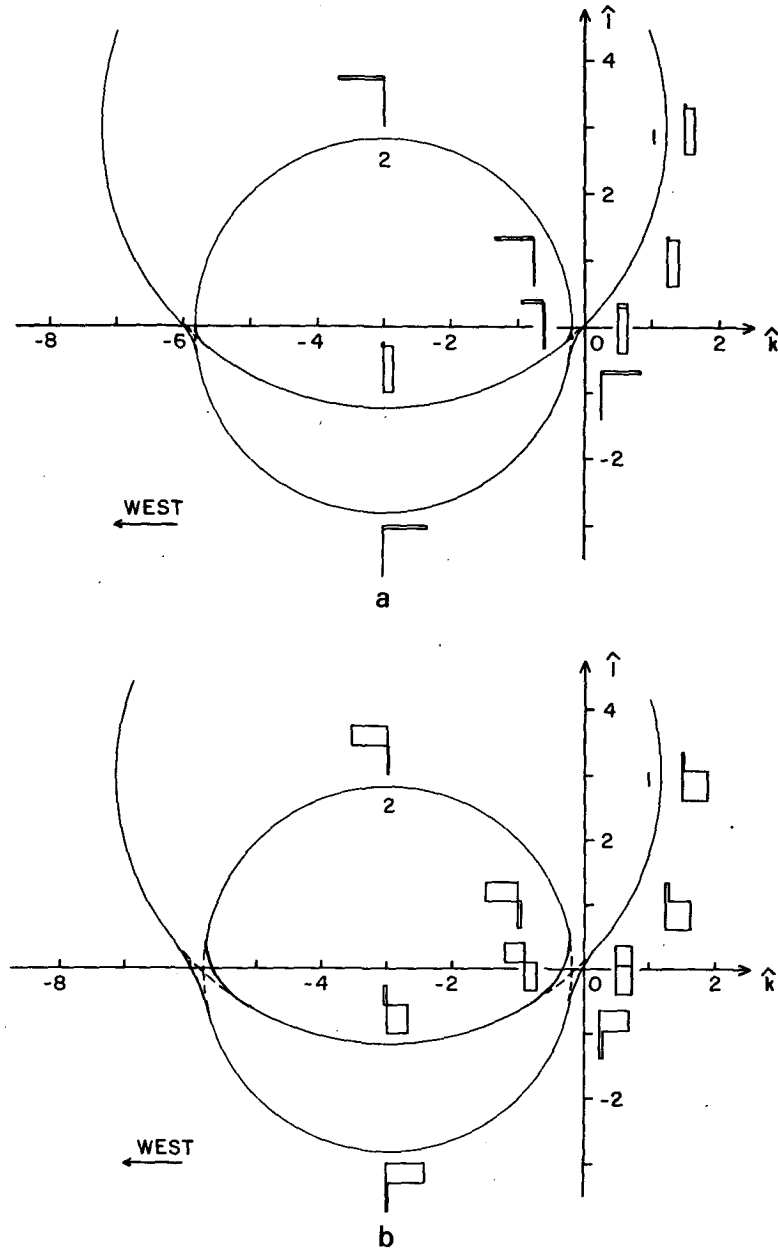


FIG. 6. Dispersion curves of the normal modes and ULC and LLC in the (k, l) plane with $\hat{\omega} = 0.002$ for $\theta = 0^\circ$: (a) $H/H' = 1/14$, (b) $H/H' = 2/3$. $\beta^T = \beta$.

necessarily mean the weakening of the effect of coupling. The effect of coupling depends on the orientation of bottom topography as well as β/β^T . For waves propagating eastward, trapping is stronger than that on an f plane for any particular wavelength.

Therefore, in some realistic circumstances, the combined effect of β and β^T gives rise to a complete decoupling between the upper and lower layers, even for waves much longer than the deformation radius. The complete decoupling obtained by Sugihara (1980) in a two-layer model with con-

tinental shelf and slope for the formation of western boundary currents may be explained by this combined effect.

Resonance takes place when the phase speeds of the ULC and LLC are identical. Occurrence of resonance is typical for a general orientation of bottom topography. The concept of resonance already has been introduced into the problem of coastal trapped waves by Kajjura (1974), Wang (1975) and Allen (1975). They try to understand waves in an ocean with both stratification and continental shelf-slope

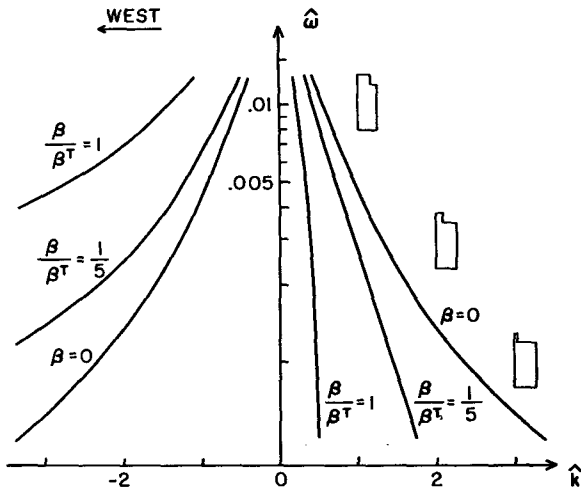


FIG. 7. Dispersion diagram of the lower layer mode with $l = 0.5$ for $\beta = 0$, $\beta/\beta^T = 1/5$ and 1 with fixed β^T ($\beta^T = \beta = 2 \times 10^{-13} \text{ cm}^{-1} \text{ s}^{-1}$) for $\theta = 0^\circ$. The deformation radius is 43.4 km at 30° latitude ($H = 500 \text{ m}$, $H' = 2500 \text{ m}$).

based on barotropic shelf waves and internal Kelvin waves. This idea has increased our knowledge of coastal trapped waves. As for the present study, the resultant resonance is a necessary consequence. The complete change in the properties of each of the normal modes is understood only as a result of the resonance. The concept of resonance will serve as a useful tool for interpreting observed phenomena such as behavior of mesoscale eddies.

The effect of bottom topography leads to properties of the normal modes similar to those of ULC and LLC. A clear understanding of the normal modes in a stratified ocean with bottom topography on a β -plane may be obtained from the use of ULC and LLC as a basic concept.

The density stratification is represented by two homogeneous layers in the present study. A two-layer model retains the essential dynamics of a stratified ocean because of the existence of a main thermocline. But, in a two-layer model, the depth of a node in vertical structure is fixed at the interface. It is worthwhile referring to the vertical structure for normal modes in a three-layer model. Actually, we consider a model in which a main thermocline is expressed by finite thickness. Results (not shown here) show that trapping by the bottom and isolation from the bottom tend to occur at the nearer interface to the bottom. These correspond to the characteristics for a continuously stratified model (Rhines, 1970). It should be repeated that the case in which a thermocline intersects the sloped bottom is not discussed for a layered model. This case, in which constraints such as a gentle slope are relaxed, needs to be studied.

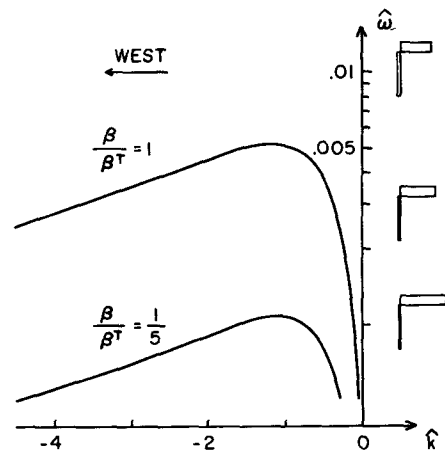


FIG. 8. Dispersion diagram of the upper layer mode with $l = 0.5$ for $\beta/\beta^T = 1/5$ and 1 with fixed β^T . Parameters are as in Fig. 7.

Direct application of the present theory to observed phenomena may be limited because the waves in a two-layer ocean with gentle, uniform slope are discussed within the scope of linear dynamics. Also, energy transfer from one layer to the other by the coupling, especially for the resonance, needs to be studied for farther application.

Acknowledgments. I would like to thank Dr. J. J. O'Brien for his encouragement and discussion. Discussions with Drs. J. Kindle, R. Krishnamurti, Y. Hsueh and J. H. Yoon were very helpful and pleasant. Thanks are extended to Drs. G. Veronis and K. Kajiuura for reading the manuscript and making very helpful comments. I thank also Mr. M. Peffley and Ms. R. Preller for refining the manuscript and Ms. S. Finney for typing the manuscript. This research in the United States was supported by the Office of Naval Research, through J. J. O'Brien at The Florida State University. This is a contribution of the Mesoscale Air-Sea Interaction Group directed by J. J. O'Brien.

REFERENCES

Allen, J. S., 1975: Coastal trapped waves in a stratified ocean. *J. Phys. Oceanogr.*, **5**, 300-325.
 Kajiuura, K., 1974: Effect of stratification on long period trapped waves on the shelf. *J. Oceanogr. Soc. Japan*, **30**, 271-281.
 Prandtl, L., 1952: *Essential of Fluid Dynamics*. Hartner, 452 pp.
 Rhines, P., 1970: Edge-, bottom-, and Rossby waves in a rotating stratified fluid. *Geophys. Fluid Dyn.*, **1**, 273-302.
 Rhines, P., 1977: The dynamics of unsteady currents. *The Sea*, Vol. 6, Interscience, Chap. 7.
 Suginohara, N., 1980: Effects of bottom topography and density stratification on the formation of western boundary currents, Part II: Inflow-outflow model. *J. Oceanogr. Soc. Japan*, **35**, 224-232.
 Wang, D. P., 1975: Coastal trapped waves in a baroclinic ocean. *J. Phys. Oceanogr.*, **5**, 326-333.